

This discussion paper is/has been under review for the journal Climate of the Past (CP).
Please refer to the corresponding final paper in CP if available.

Water mass evolution of the Greenland Sea since lateglacial times

M. M. Telesiński¹, R. F. Spielhagen^{1,2}, and H. A. Bauch^{1,2}

¹GEOMAR Helmholtz Centre for Ocean Research Kiel, Wischhofstrasse 1–3,
24148 Kiel, Germany

²Academy of Sciences, Humanities, and Literature, 53151 Mainz, Germany

Received: 15 August 2013 – Accepted: 21 August 2013 – Published: 30 August 2013

Correspondence to: M. M. Telesiński (mtelesinski@geomar.de)

Published by Copernicus Publications on behalf of the European Geosciences Union.

Water mass evolution of the Greenland Sea since lateglacial times

M. M. Telesiński et al.

[Title Page](#)

[Abstract](#)

[Introduction](#)

[Conclusions](#)

[References](#)

[Tables](#)

[Figures](#)

[⏪](#)

[⏩](#)

[◀](#)

[▶](#)

[Back](#)

[Close](#)

[Full Screen / Esc](#)

[Printer-friendly Version](#)

[Interactive Discussion](#)

Abstract

Four sediment cores from the central and northern Greenland Sea, a crucial area for the global ocean circulation system, were analyzed for planktic foraminiferal fauna, planktic and benthic stable oxygen and carbon isotopes as well as ice-rafted debris. During the Last Glacial Maximum, the Greenland Sea was dominated by cold and ice-bearing water masses. Meltwater discharges from the surrounding ice sheets affected the area during the deglaciation, influencing the water mass circulation. The Younger Dryas was the last major freshwater event in the area. The onset of the Holocene interglacial was marked by an improvement of the environmental conditions and rising sea surface temperatures (SST). Although the thermal maximum was not reached simultaneously across the basin, due to the reorganization of the specific water mass configuration, benthic isotope data indicate that the overturning circulation reached a maximum in the central Greenland Sea around 7 ka. After 6–5 ka the SST cooling and increasing sea-ice cover is noted alongside with decreasing insolation. Conditions during this Neoglacial cooling, however, changed after 3 ka due to further sea-ice expansion which limited the deep convection. As a result, a well stratified upper water column amplified the warming of the subsurface waters in the central Greenland Sea which were fed by increased inflow of Atlantic Water from the eastern Nordic Seas. Our data reconstruct a variety of time- and space-dependent oceanographic conditions. These were the result of a complex interplay between overruling factors such as changing insolation, the relative influence of Atlantic, Polar and meltwater, sea-ice processes and deep water convection.

1 Introduction

The Nordic Seas are an important region for the global oceanic system. First of all, they are the main gateway between the Arctic and North Atlantic oceans (Hansen and Østerhus, 2000). They also play a fundamental role in the overturning circulation

CPD

9, 5037–5075, 2013

Water mass evolution of the Greenland Sea since lateglacial times

M. M. Telesiński et al.

[Title Page](#)

[Abstract](#)

[Introduction](#)

[Conclusions](#)

[References](#)

[Tables](#)

[Figures](#)

[⏪](#)

[⏩](#)

[◀](#)

[▶](#)

[Back](#)

[Close](#)

[Full Screen / Esc](#)

[Printer-friendly Version](#)

[Interactive Discussion](#)



Water mass evolution of the Greenland Sea since lateglacial times

M. M. Telesiński et al.

[Title Page](#)

[Abstract](#)

[Introduction](#)

[Conclusions](#)

[References](#)

[Tables](#)

[Figures](#)

[⏪](#)

[⏩](#)

[◀](#)

[▶](#)

[Back](#)

[Close](#)

[Full Screen / Esc](#)

[Printer-friendly Version](#)

[Interactive Discussion](#)



time cold, low-saline ($< 0^{\circ}\text{C}$, < 34.4) Polar Water (PW) flows south through the Fram Strait and along the Greenland continental margin to enter the North Atlantic through the Danish Strait. The strong gradient between these two main surface water masses makes the Nordic Seas sensitive to any oceanographic changes in time. The central part of the Nordic Seas is the domain of Arctic Water (ArW), a result of PW and AW mixing (Swift, 1986). ArW is separated from PW by the Polar Front and from AW by the Arctic Front.

Finally, the Nordic Seas are one of the areas where deep water convection and the formation of North Atlantic Deep Water (NADW) take place (e.g. Marshall and Schott, 1999). The western branches of the NAC and the eastern branches of the East Greenland Current (EGC) create the cyclonic circulation in the Greenland Sea and lead to doming of the water layers. As the two water masses mix together, they increase their density and sink to the bottom (Hansen and Østerhus, 2000). Subsequently the water leaves the Nordic Seas as the Denmark Strait and Island-Scotland Overflow Water (DSOW and ISOW, respectively).

Sea-ice plays an important preconditioning role in the Greenland Sea compared to other convectional areas. In early winter the spreading sea-ice leads to the brine rejection. The surface layer increases its density and sinks to about 150 m by mid-January. Preconditioning continues later in the winter with mixed-layer deepening in the ice-free area (Nord Bukta) to 300–400 m, induced by strong winds blown over the ice. Finally, typically in March, preconditioning is advanced enough to develop deep convection (down to > 2000 m) in the Greenland Sea, if the meteorological conditions are favorable (Marshall and Schott, 1999).

The vertical structure of the water column in the central Greenland Sea consists of three layers. At the surface, there is a thin layer of Arctic Surface Water originating from the EGC. Underneath, a layer of Atlantic Intermediate Water exists supplied from the NAC. The weekly stratified Greenland Sea Deep Water, the product of deep convection, is found below (Marshall and Schott, 1999).

Water mass evolution of the Greenland Sea since lateglacial times

M. M. Telesiński et al.

[Title Page](#)

[Abstract](#)

[Introduction](#)

[Conclusions](#)

[References](#)

[Tables](#)

[Figures](#)

[⏪](#)

[⏩](#)

[◀](#)

[▶](#)

[Back](#)

[Close](#)

[Full Screen / Esc](#)

[Printer-friendly Version](#)

[Interactive Discussion](#)



At present, the sites investigated in this study are all located within the ArW domain. A detailed description of site PS1878 was given by Telesiński et al. (2013). The three sites from the northern Greenland Sea, PS1894, PS1906 and PS1910, are located on the Greenland continental slope, on the northern and on the southern part of the Greenland Fracture Zone crest, respectively.

3 Material and methods

The sediment cores used in this study were retrieved during the ARK-VII/1 expedition of RV *Polarstern* in 1990. Core PS1878 is compiled from a giant box core PS1878-2 and a kasten core PS1878-3 (Telesiński et al., 2013), whereas the three others are giant box cores (Table 1). All cores consisted of brown to olive grey sediments of clay to silty sand. They were sampled continuously every 1 cm. Additionally, surface sediments of cores PS1894, PS1906 and PS1910 were collected. Further preparation included freeze-drying, wet-sieving with deionized water through a 63 μm mesh, and dry-sieving into size fractions using 100, 125, 250, 500 and 1000 μm sieves. Each size fraction was weighted.

In the representative splits (> 300 specimens) of the 100–250 μm size fraction planktic foraminifera were counted. Samples containing less than 100 specimens were not used for the relative species abundance analysis. The number of planktic foraminifera per 1 g dry sediment was calculated.

The identification and counting of several mineral grains types > 250 μm was used as a proxy for the intensity of ice-rafting and identification of tephra layers. As IRD we interpret all the lithic grains > 250 μm (except for unweathered volcanic glass). In the high latitudes, such coarse particles can be transported into a deep ocean basin preferentially by icebergs while sea-ice mainly transports finer material (Clark and Hanson, 1983; Nürnberg et al., 1994).

For the analysis of stable oxygen and carbon isotopes, a planktic species *Neoglobobadrina pachyderma* (sin.) (all cores) and two benthic species – the epibenthic *Cibi-*

Water mass evolution of the Greenland Sea since lateglacial times

M. M. Telesiński et al.

Title Page

Abstract

Introduction

Conclusions

References

Tables

Figures

⏪

⏩

◀

▶

Back

Close

Full Screen / Esc

Printer-friendly Version

Interactive Discussion

cidoides wuellerstorfi and the shallow infaunal *Oridorsalis umbonatus* (cores PS1894, PS1910 and PS1878) were used. Because of the well-known departure from isotopic calcite equilibrium, the measured $\delta^{18}\text{O}$ values of both benthic species were corrected by +0.64 and +0.36‰, respectively (Duplessy et al., 1988). Twenty five specimens were picked from the 125–250 μm (*N. pachyderma* (sin.) and *O. umbonatus*) or 250–500 μm (*C. wuellerstorfi*) size fractions. All stable isotope analyses were carried out in the isotope laboratory of GEOMAR. Results are expressed in the δ notation referring to the PDB standard and are given as $\delta^{18}\text{O}$ and $\delta^{13}\text{C}$.

Absolute summer subsurface temperatures (100 m water depth) were calculated at site PS1878 between 15 and 0 ka using transfer functions based on a modern training set from the Arctic (Husum and Hald, 2012) and the C2 software, version 1.7.2 (Juggins, 2011). A Weighted Average Partial Least-Squares statistical model with three components (WAP-LS C3) was used. Cross validation was provided with leave-one-out (“jack knifing”). The Root Mean-Squared Error of Prediction is 0.52 °C. Unlike Husum and Hald (2012), who used the > 100 μm size fraction, we ran the transfer function using the 100–250 μm size fraction. Although the coarser sediments contained relatively few foraminifera we acknowledge that this might have slightly biased the results. Further, reconstructed temperatures below 2 °C are considered to be uncertain as the modern training set does contain very few data points below 2 °C (Husum and Hald, 2012).

4 Chronology

AMS ^{14}C datings were performed on monospecific samples of *N. pachyderma* (sin.) (Table 2). All radiocarbon ages were corrected for a reservoir age of 400 yr, calibrated using Calib Rev 6.1.0 software (Stuiver and Reimer, 1993) and the Marine09 calibration curve (Reimer et al., 2009) and are given in thousand calendar years before 1950 CE (ka).

2003) that we used for the correlation. A trend towards lower $\delta^{18}\text{O}$ values commences thereafter and lasts until the end of the record. A distinct, though irregular, variability can be observed within the trend (Figs. 2 and 5).

5 The oldest part of all planktic carbon isotope records (> 18 ka) exhibits low and stable values around 0.0–0.3‰. Simultaneous with the light $\delta^{18}\text{O}$ peaks the $\delta^{13}\text{C}$ values decrease slightly and a trend of increasing values commences thereafter. Around 7 ka the $\delta^{13}\text{C}$ values reach a high plateau of 0.7–1.0‰, which lasts until 3 ka and ends with a relatively sudden drop.

10 In the lowermost parts of our cores the benthic species *O. umbonatus* and *C. wuellerstorfi* were partly absent. Therefore we can present here only the last 16 kyr of the benthic stable isotope records (Fig. 6). The oxygen isotope ratios of both benthic species generally show a decreasing trend parallel to the planktic record with values ca. 0.7–1.0‰ heavier than those of *N. pachyderma* (sin). The epibenthic (*C. wuellerstorfi*) $\delta^{13}\text{C}$ records also parallel the planktic curves in terms of the main features, but the values are 0.2–1.0‰ higher and the changes are of lower amplitude. The only major exception is the youngest (< 3 ka) part of record PS1894 in which the benthic $\delta^{13}\text{C}$ continue to rise slightly despite the decrease in the planktic record.

5.3 Subsurface temperature reconstruction

20 The subsurface temperature record of core PS1878 shows values steadily increasing from around 2°C around 15 ka to a maximum of 3–3.5°C between 8 and 5.7 ka (Fig. 7). Thereafter it decreases stepwise to values around 2°C between 3.8 and 2.3 ka. Subsequently the record shows rapidly increasing temperatures with a peak value of ca. 3.5°C at 1.3 ka and a decrease to ca. 3°C thereafter.

Water mass evolution of the Greenland Sea since lateglacial times

M. M. Telesiński et al.

Title Page

Abstract

Introduction

Conclusions

References

Tables

Figures

⏪

⏩

◀

▶

Back

Close

Full Screen / Esc

Printer-friendly Version

Interactive Discussion

6 Discussion

6.1 Last glacial maximum (LGM)

Our Greenland Sea $\delta^{18}\text{O}$ records begin with heavy values of $> 4.5\text{‰}$ (Fig. 2) which were found earlier to be typical for the late glacial maximum in the Nordic Seas and Fram Strait indicative of high salinity AW advected to the north (Sarnthein et al., 1995; Nørgaard-Pedersen et al., 2003). The low foraminiferal abundance and species diversity (Figs. 3 and 4) are evidence of a low biological productivity in the Greenland Sea during the LGM. The latter might be a result of the result of the perennial sea-ice cover that would strongly limit the penetration of sunlight and reduce the growth of phytoplankton that the foraminifera feed on. Furthermore, the sea-ice cover would lower the gas exchange between the ocean and the atmosphere.

Low $\delta^{13}\text{C}$ might suggest that the foraminifera lived in a poorly ventilated subsurface water layer (cf. Duplessy et al, 1988) which would support the perennial sea-ice cover. However, in the perennially ice-covered areas like the central Arctic Ocean relatively high $\delta^{13}\text{C}$ values ($> 0.7\text{‰}$) are found at present (Spielhagen and Erlenkeuser, 1994). Therefore we do not relate the low $\delta^{13}\text{C}$ to the sea-ice and/or strong stratification of the upper water layers. The carbon cycle in the glacial ocean could have been much different than at present. Therefore it is difficult to unambiguously interpret the carbon isotope record in this interval.

The LGM sediments, especially in cores PS1906 and PS1910, contain high amounts of coarse ice-rafted debris compared to younger layers (Fig. 3). This indicates numerous icebergs passing the area and losing transported material. The IRD concentration is highly variable and marked with numerous prominent peaks. In cores PS1906, PS1894 and PS1878 they clearly coincide with foraminiferal abundance peaks. As already discussed by Telesiński et al. (2013) for site PS1878, these peaks may represent sporadic and relatively short intervals of somewhat ameliorated conditions during which the decreased sea-ice occurrence and slightly warmer surface water resulted in higher biological productivity, increased IRD delivery and, as a result, higher sedimentation

Water mass evolution of the Greenland Sea since lateglacial times

M. M. Telesiński et al.

Title Page

Abstract

Introduction

Conclusions

References

Tables

Figures

⏪

⏩

◀

▶

Back

Close

Full Screen / Esc

Printer-friendly Version

Interactive Discussion



rates. Thus, the duration of these intervals may be overrepresented in the sediment record, the most compelling example being the IRD and foraminiferal peaks in core PS1906 at ca. 25–30 cm. Variable sedimentation rates and the uncertainties in our age models for the LGM make it difficult to say whether the ameliorated conditions occurred basinwide or were regionally diachronous.

6.2 Deglaciation

Prominent low $\delta^{18}\text{O}$ peaks accompanied by low $\delta^{13}\text{C}$ values are recorded in the deglacial parts of cores PS1878 and PS1906, as well as PS1230 (Bauch et al., 2001) and PS2887 (Nørgaard-Pedersen et al., 2003). Similar, though more obscure features can be traced in cores PS1894 and PS1910 (Fig. 2). We interpret them as a result of the discharge of isotopically light freshwater that lowered the regional surface water salinity (Sarnthein et al., 1995; Spielhagen et al., 2004; Telesiński et al., 2013). In cores PS1906 and PS1878 the high amplitude of the $\delta^{18}\text{O}$ peaks together with low IRD abundance in the respective intervals suggest that the freshwater originated from catastrophic freshwater discharges from terrestrial sources (e.g. outbursts from ice-dammed or subglacial lakes) rather than from a delivery by melting glaciers or icebergs.

The significant thickness of the light $\delta^{18}\text{O}$ layers in cores PS1878 and PS2887 indicates that in some cases during the freshwater discharges the sedimentation rates increased dramatically as we assume that a freshwater outburst cannot last incessantly for several thousand years. This suggests that the discharged freshwater might have been loaded with fine-grained sediments that were subsequently deposited in a relatively short period of time. However, even freshwater loaded with sediments would travel along a basin floor as a hyperpycnal flow and would not directly affect the planktic $\delta^{18}\text{O}$ record (Stanford et al., 2011). Therefore, if the freshwater discharges at sites PS1878 and PS2887 were indeed loaded with sediments, they had to be accompanied by sediment-free freshwater outbursts that directly affected the planktic record.

Water mass evolution of the Greenland Sea since lateglacial times

M. M. Telesiński et al.

Title Page

Abstract

Introduction

Conclusions

References

Tables

Figures

⏪

⏩

◀

▶

Back

Close

Full Screen / Esc

Printer-friendly Version

Interactive Discussion



Water mass evolution of the Greenland Sea since lateglacial times

M. M. Telesiński et al.

[Title Page](#)

[Abstract](#)

[Introduction](#)

[Conclusions](#)

[References](#)

[Tables](#)

[Figures](#)

[⏪](#)

[⏩](#)

[◀](#)

[▶](#)

[Back](#)

[Close](#)

[Full Screen / Esc](#)

[Printer-friendly Version](#)

[Interactive Discussion](#)

On the other hand, the well-dated core PS2887 (Nørgaard-Pedersen et al., 2003) indicates the extent of the low $\delta^{18}\text{O}$ spike of more than 2 kyr and the interpolated age of the spike in PS1878 (18–15 ka) fits well with the duration of the Heinrich stadial 1 (HS1). These arguments suggest that the freshwater could have been present in the Greenland Sea for several thousand years and the low foraminiferal abundance during that time might be a result of the salinity decrease below the level tolerated by the foraminifers while the lack of IRD might be caused by the decrease in icebergs mobility and melt rate due to the increased presence of sea-ice.

The reservoir ages during the deglaciation, especially in case of massive freshwater discharges that were able to influence the oceanic circulation significantly, remain highly uncertain and may have been larger than 1000 yr (Waelbroeck et al., 2001; Stern and Lisiecki, 2013). Additionally, low sedimentation rates in some of the cores make the age model based on AMS ^{14}C datings to a large extent speculative. Therefore we find it reasonable to argue that the major deglacial freshwater discharges in the western Nordic Seas occurred roughly simultaneously, as was previously suggested by Telesiński et al. (2013). The most obvious mechanism to trigger the discharges over such a large area seems to be the sea level rise which started shortly after 20 ka (Clark and Mix, 2002).

All our records show low carbon isotope ratios during the proposed freshwater events (Fig. 2), indicating that the ventilation of the (sub)surface water was even weaker than during the LGM in most of the Greenland Sea (cf. Sarnthein et al., 1995; Spielhagen et al., 2004). During these freshwater events the water column stratification must have been enhanced as the low-salinity water has lower density and creates a stable lid on top of the water column. If the stratification was a basin wide phenomenon as shown by our records, it seems to support the previous suggestions (Stanford et al., 2011; Telesiński et al., 2013) of the Atlantic Meridional Overturning Circulation (AMOC) slow-down during HS1 and gives a rough chronological framework for the onset of the deglaciation.

**Water mass evolution
of the Greenland Sea
since lateglacial
times**

M. M. Telesiński et al.

[Title Page](#)[Abstract](#)[Introduction](#)[Conclusions](#)[References](#)[Tables](#)[Figures](#)[⏪](#)[⏩](#)[◀](#)[▶](#)[Back](#)[Close](#)[Full Screen / Esc](#)[Printer-friendly Version](#)[Interactive Discussion](#)

Our benthic oxygen isotope records do not cover the initial part of H1 (Fig. 6). However, around 15.5–15.0 ka the PS1878 record of *O. umbonatus* shows a distinct decrease in the $\delta^{18}\text{O}$ values, though of much lower amplitude than in the planktic record. This could suggest that the (somewhat diluted) low $\delta^{18}\text{O}$ signal from the surface reached down to the bottom of the water column. According to Hillaire-Marcel and de Vernal (2008), the formation of sea-ice from low salinity, low temperature and low $\delta^{18}\text{O}$ surface water could result in the production of isotopically light brines. Stanford et al. (2011) reject such a hypothesis, finding it unlikely that brines formed from freshwater could sink to intermediate depths (see also Rasmussen and Thomsen, 2009; Bauch and Bauch, 2001), not to mention the bottom of a deep basin at which our site is located. Instead, Stanford et al. (2011) propose a different explanation for the occurrence of light $\delta^{18}\text{O}$ excursions during HS1. They suggest that meltwater loaded with sediments entered the Nordic Seas below the sea surface as a hyperpycnal flow. In our record, the negative benthic $\delta^{18}\text{O}$ excursion at 15.5–15.0 ka may result from such a mechanism. However, in the record studied by Stanford et al. (2011), the benthic oxygen isotope depletion has an amplitude larger than the planktic record, which is not observed in our record. Stanford et al. (2011) explain that, after losing the sediment load, the remaining relatively fresh, low density and low $\delta^{18}\text{O}$ water rose towards the surface (while strongly mixing with ambient water) resulting in the amplitude difference. This seems not to be the case in our record. Possibly the freshwater event in or close to the Greenland Sea released both a sediment-loaded and a largely sediment-free freshwater plume which in combination may explain the strong near-surface and weaker bottom water $\delta^{18}\text{O}$ depletions. The sediment-loaded plume mechanism may also explain the significant thickness of the light $\delta^{18}\text{O}$ layers in cores PS1878 and PS2887. While the plume was losing its load, the sedimentation rates increased dramatically in the affected areas resulting in thick, fine-grained deposits. The duration of the freshwater outbursts was significantly shorter than it appears from the linear age interpolation between the dating points as such an event cannot last incessantly for several thousand years.

Following the freshwater event(s), the planktic $\delta^{18}\text{O}$ values increased to values around 4‰ or more (Figs. 2 and 5), indicating that the freshwater influence had decreased by this time. Also the increasing $\delta^{13}\text{C}$ values suggest that the ventilation of (at least subsurface) water was reactivated.

In the PS1910 record, changes in the oxygen isotope record are gradual and of low amplitude. This suggests that the site was not directly influenced by freshwater discharges. Short freshwater events like those recorded in core PS1878 between 15 and 13 ka may have taken place at site PS1910 (as well as PS1906 after the major event) but are obscured by low resolution. The generally heavy $\delta^{18}\text{O}$ values throughout the deglaciation, as well as later on, indicate a relatively strong inflow of Atlantic waters to this area.

Core PS1894 recorded generally the lowest planktic $\delta^{18}\text{O}$ values of all four records. This site is located on the Greenland continental slope, in direct proximity to the EGC and under the sea-ice cover. Thus the lowest $\delta^{18}\text{O}$ might result from the weakest influence of AW and the lowest salinity. Today, the salinity at site PS1894 is 1–2 lower than further to the east, in the ice-free areas (Thiede and Hempel, 1991). In contrast to the other sites, the onset of the deglaciation (after 17 ka) seems to be characterized by a warming of the (sub)surface water rather than by a freshwater inflow, as the oxygen isotope ratio decrease is accompanied by the appearance of subpolar foraminiferal species (Figs. 2 and 4). It is possible that a minor enhancement of the Atlantic Water inflow into the north-western Greenland Sea coincided with and probably also contributed to the termination of LGM-type conditions and the onset of deglacial changes at this site. It might seem counterintuitive that at this site which is the one most affected by PW, the subpolar species appeared so early and in such high amounts (around 20%), especially since even in late Holocene sediments they constitute less than 20% of the planktic fauna in this area (Husum and Hald, 2012). It may, however, indicate the advection of Atlantic waters subducted below stratified and sea-ice covered surface water layers (Bauch et al., 2001). This is confirmed by the modern oceanographic measurements on a W–E profile across the Greenland Sea (Thiede and Hempel, 1991)

Water mass evolution of the Greenland Sea since lateglacial times

M. M. Telesiński et al.

[Title Page](#)[Abstract](#)[Introduction](#)[Conclusions](#)[References](#)[Tables](#)[Figures](#)[⏪](#)[⏩](#)[◀](#)[▶](#)[Back](#)[Close](#)[Full Screen / Esc](#)[Printer-friendly Version](#)[Interactive Discussion](#)

showing higher subsurface temperatures at stations covered with sea-ice than in the ice-free areas.

After the initial decrease in $\delta^{18}\text{O}$, the values in the PS1894 record remain lower than at other sites (Fig. 2). Although the data do not indicate any major direct freshwater discharges in this area, the surface water salinity was apparently lower than at the other sites, probably as a result of the proximity of the ice margin and the EGC.

6.3 Younger Dryas (YD)

Only core PS1878 contains a clear light $\delta^{18}\text{O}$ excursion (12.8–11.9 ka) that fits into the timespan of the YD (12.9–11.7 ka, cf. Broecker et al., 2010). However, less prominent oxygen isotope peaks of the same age can be found in cores PS1906 and PS1910, as well as in PS1230 and PS1243 (Bauch et al., 2001). We associate them also with the YD and used them for the correlation of the cores (Figs. 2 and 5). The oxygen isotope record of core PS1894 contains no indications that could be linked to the YD. However, as already mentioned above, this record exhibits generally low $\delta^{18}\text{O}$ values ($< 3.5\text{‰}$ in the interval around the YD), often lower than those of the light $\delta^{18}\text{O}$ excursions in the other records. This indicates that the site was under a constant influence of relatively fresh PW that could obscure the YD signal.

The debate on the origin, nature and course of the YD continues for decades (e.g. Broecker et al., 1989, 2010; Teller et al., 2005; Murton et al., 2010; Fisher and Lowell, 2012) and certainly the last word has not been spoken yet. We do not aim to solve this issue. However, the presence of the YD light $\delta^{18}\text{O}$ signal in the Fram Strait and the Greenland Sea suggests the Arctic region as the source area for the freshwater pulse. If such a pulse was indeed the trigger for the YD (cf. Broecker et al., 2010), then our data would support the modeling results of Condron and Winsor (2012). They indicate that only a freshwater discharge to the Arctic (probably via the Mackenzie Valley) was able to reach the deepwater formation regions in the North Atlantic (including our study area) and weaken the AMOC sufficiently to trigger the YD.

Water mass evolution of the Greenland Sea since lateglacial times

M. M. Telesiński et al.

Title Page

Abstract

Introduction

Conclusions

References

Tables

Figures

⏪

⏩

◀

▶

Back

Close

Full Screen / Esc

Printer-friendly Version

Interactive Discussion



proximity of the Transpolar Drift, still bringing numerous icebergs from the circum-Arctic region.

Site PS1894 showed the least significant changes at the onset of the Holocene. The abundance of subpolar fauna only recovered from a slight decrease during the YD (Fig. 9). The increase in faunal abundance was more significant but it reached only around half of its Holocene maximum (Fig. 8). In contrast to the other sites, the IRD abundance increased and remained positively correlated with the foraminiferal abundance. These proxy data indicate that the eastern part of the Greenland Sea remained under the polar conditions with cold surface water, numerous icebergs and sea-ice cover presumably for most of the time.

For the entire study area, it is difficult to define a common thermal maximum which we define as the interval with the highest percentage of subpolar species (or highest absolute temperatures in core PS1878). Not only the course of the initial warming but also the duration and the termination of the warmest interval differed between the sites. In the southern Fram Strait (site PS1906) the thermal maximum started already around 11.5 ka and ended gradually between 7 and 3 ka. At sites PS1894, PS1910 and PS1878 it was significantly shorter and can be dated to ca. 11–9.5, 10.5–7 and 8–5.5 ka, respectively. This might at least partly be attributed to the uncertainties in the correlation between the records which was mainly based on the isotope records. Nevertheless, the onset of the warmest interval around 11–9 ka accords with many other Nordic Seas records (e.g. Bauch et al., 2001; Sarnthein et al., 2003; Giraudeau et al., 2010; Risebrobakken et al., 2011; Husum and Hald, 2012) where the beginning of the Holocene Thermal Maximum (HTM) was related to maximum insolation in the high latitudes (e.g. Andersen et al., 2004; Risebrobakken et al., 2011) and the maximum in northward oceanic heat transport by the NAC (Risebrobakken et al., 2011). The late thermal maximum at site PS1878 might have resulted from the large distance between the site and the core of the NAC (Fig. 1) as well as the presence of freshwater in the earliest Holocene (Fig. 5) though the latter must be expected also for the other three sites. Also the relative proximity of the remnant Greenland Ice Sheet, still deliv-

Water mass evolution of the Greenland Sea since lateglacial times

M. M. Telesiński et al.

[Title Page](#)

[Abstract](#)

[Introduction](#)

[Conclusions](#)

[References](#)

[Tables](#)

[Figures](#)



[Back](#)

[Close](#)

[Full Screen / Esc](#)

[Printer-friendly Version](#)

[Interactive Discussion](#)



Water mass evolution of the Greenland Sea since lateglacial times

M. M. Telesiński et al.

[Title Page](#)

[Abstract](#)

[Introduction](#)

[Conclusions](#)

[References](#)

[Tables](#)

[Figures](#)

[⏪](#)

[⏩](#)

[◀](#)

[▶](#)

[Back](#)

[Close](#)

[Full Screen / Esc](#)

[Printer-friendly Version](#)

[Interactive Discussion](#)

Weinelt, 1997). Its onset also corresponds to the establishment of the modern ISOW flow (Thornalley et al., 2010) and AMOC strengthening (Hall et al., 2004). Our benthic $\delta^{13}\text{C}$ records (Fig. 6) as well as other benthic records from the Nordic Seas (Bauch et al., 2001; Sarnthein et al., 2003) also exhibit relatively high values in this interval. This implies good ventilation of the bottom water and together with the above mentioned data suggests that between 7 and 3 ka intensive deep water convection took place in the Nordic Seas. The AMOC intensification after 7 ka implies enhanced inflow of AW and PW into the Greenland Sea. The increasing influence of cold PW would amplify the Neoglacial cooling in the area which might explain the relatively sharp warm-cold transition at site PS1878 at 5.5 ka. The cooling, in turn, would enhance the sea-ice formation and strong winds which would open up leads and provoke super-cooling processes further intensifying the deep water formation.

Our central Greenland Sea record (PS1878) shows benthic $\delta^{13}\text{C}$ values $> 1.5\text{‰}$ which are unequalled if compared to other Holocene records from the Nordic Seas (Fig. 6, cf. Bauch et al., 2001; Sarnthein et al., 2003). This indicates that the bottom water was well ventilated. The only process that could explain it is the deep convection. Therefore our data suggest that the deep convection was taking place in the central Greenland Sea, in the proximity of site PS1878 and it was at its maximum between 7 and 3 ka.

The planktic $\delta^{13}\text{C}$ decrease after around 3 ka, observed in all our records (Fig. 5), appears to be a sound stratigraphic time marker (Bauch and Weinelt, 1997). Moreover, as it occurs in all our records from the western Nordic Seas as well as in sediment cores from the eastern Nordic Seas (e.g. Vogelsang, 1990; Fronval and Jansen, 1997; Bauch et al., 2001; Sarnthein et al., 2003; Risebrobakken et al., 2011; Werner et al., 2013) this event is of overregional implication. We relate these changes to a decrease in ventilation of the subsurface water and an increase in stratification of the upper water layers. A reconstruction of sea-ice conditions in the Fram Strait (Müller et al., 2012) showed increasing sea-ice occurrences since 8 ka. Around 3 ka a further significant expansion of sea-ice cover occurred and the sea-ice conditions became more fluctuating.

Water mass evolution of the Greenland Sea since lateglacial times

M. M. Telesiński et al.

[Title Page](#)

[Abstract](#)

[Introduction](#)

[Conclusions](#)

[References](#)

[Tables](#)

[Figures](#)

[⏪](#)

[⏩](#)

[◀](#)

[▶](#)

[Back](#)

[Close](#)

[Full Screen / Esc](#)

[Printer-friendly Version](#)

[Interactive Discussion](#)

Although in the record from the East Greenland Shelf (Müller et al., 2012) no increase in sea-ice cover is observed before 3 ka (perhaps because this area was strongly influenced by the sea-ice during the entire Holocene), the total sea-ice cover in the Nordic Seas was probably increasing. Renssen et al. (2006) showed that negative solar irradiance anomalies can cause an expansion of sea-ice temporarily relocating deepwater formation sites in the Nordic Seas. One of the strongest anomalies in the Holocene occurred between 2.85 and 2.6 ka and could have triggered the sudden increase in sea-ice extent, increased the stratification of the upper water layers and decreased the ventilation of the subsurface water. This solar irradiance anomaly may also be related to the increase in ice-rafting in the North Atlantic around that time (Bond et al., 2001; Renssen et al., 2006).

In two of our benthic carbon isotope records (PS1910 and PS1878, Fig. 6) we observe a decrease around 3 ka similar to that in the planktic record. This is, however, not the case elsewhere (PS1894; Bauch et al., 2001; Sarnthein et al., 2003; Werner et al., 2013). The decrease in the benthic $\delta^{13}\text{C}$ values suggests that, probably as a result of the more extensive sea-ice cover and a stronger stratification of the upper water layers, deep convection diminished or did not reach the maximum basin depth anymore (Renssen et al., 2006). The two sites (PS1910 and PS1878) were most probably located closest to the convection centre and the decrease in convection rate or depth was recorded there as the benthic $\delta^{13}\text{C}$ decrease. At other sites that were located farther from the convection centre the bottom waters were not as well ventilated before 3 ka and therefore there was no decrease in their ventilation that would be large enough to be recorded in the sediment archive.

As described by Telesiński et al. (2013), significant changes are observed in core PS1878 since 3 ka. The total foraminiferal abundance (Fig. 8) and percentage of sub-polar species (Fig. 9) increase and the planktic carbon and oxygen isotope ratios decrease. These changes were interpreted as warming of subsurface water caused by the NAO-induced increase in the AW inflow amplified by stronger upper water layers stratification (Telesiński et al., 2013). The benthic data from core PS1878 show that the

planktic and two benthic oxygen isotope records, which in the older part of the record ran roughly parallel to each other, diverge after 3 ka (Figs. 5 and 6). The planktic values begin to decrease after the stable interval of the Middle Holocene and *O. umbonatus* values start to increase, while *C. wuellerstorfi* oxygen isotope ratios follow the earlier slightly decreasing trend. This indicates increasing differentiation of water masses and fits well with the previous interpretation.

In the other records from the Greenland Sea the changes after 3 ka are not that obvious. Core PS1894 shows a slight increase in the percentage of subpolar species (Fig. 9) and an increase in the total faunal abundance and IRD (Fig. 8). At this location, strongly affected by the PW, this might indicate at least seasonally open water conditions with somewhat higher temperatures at the surface (a situation similar to that at other sites during the LGM, see above). Planktic oxygen isotope ratios decrease slightly which might suggest warming of the subsurface water. Cores PS1906 and PS1910 show virtually no indications of warming or increased AW influence.

The subsurface temperature reconstruction from site PS1878 indicates a warming from ca. 2°C at 2.5 ka to 3.5°C at 1.5 ka, confirming that conditions in the central Greenland Sea in the Late Holocene were comparable to the Early Holocene warm interval (cf. Telesiński et al., 2013). The scale of this warming (1.5°C) is comparable to that of the modern warming in the Arctic (e.g. Spielhagen et al., 2011) though of course on a significantly longer time scale. A comparison with the faunal data from other Greenland Sea cores (Fig. 9) shows that this phenomenon was confined only to the central part of the Greenland Sea and resulted from the co-occurrence of the stronger water column stratification and the enhanced inflow of Atlantic waters to the site.

Water mass evolution of the Greenland Sea since lateglacial times

M. M. Telesiński et al.

[Title Page](#)[Abstract](#)[Introduction](#)[Conclusions](#)[References](#)[Tables](#)[Figures](#)[⏪](#)[⏩](#)[◀](#)[▶](#)[Back](#)[Close](#)[Full Screen / Esc](#)[Printer-friendly Version](#)[Interactive Discussion](#)

7 Summary and conclusions

The records presented here show the first millennial- to multicentennial-scale image of the paleoceanographic evolution in the northern and central Greenland Sea. Despite the low sedimentation rates in the northern part of the study area and the related chronological uncertainties, the correlation and comparison with a high resolution record PS1878 (Telesiński et al., 2013) allowed us to study the spatial and temporal range of the most important oceanographic processes. The integration of surface, sub-surface and bottom water proxies gave an almost complete image.

During the LGM environmental conditions were to a large extent similar across the Greenland Sea. Cold conditions with abundant sea-ice, numerous icebergs and low biological productivity prevailed in the area. During the deglaciation the Greenland Sea was affected by freshwater discharges. Although we argue that they were roughly simultaneous (between 18 and 15 ka) and had a common trigger mechanism, their sources and character were probably different. During the YD the Greenland Sea was affected by a major deglacial freshwater discharge most probably originating from the Arctic. Our data suggest a thicker but weaker halocline, better ventilation of the subsurface water and a deepening of AW.

The onset, duration and decline of the Early Holocene warm interval were apparently different in age and scale at each site reflecting the reorganization of the ocean circulation in the region. Similarly, the peak warming was not reached simultaneously at all sites. The thermal maximum at site PS1878 was not reached until ca. 8 ka which is late compared to other Nordic Seas records. Maximum subsurface temperatures ($> 3^{\circ}\text{C}$) were higher than at present, indicating a strong influence of Atlantic waters. Since 7 ka high $\delta^{13}\text{C}$ values, both planktic and benthic, indicate the establishment of the modern ocean circulation in the Nordic Seas with maximum deep convection in the Greenland Sea. Despite the strong AMOC, decreasing insolation led to the Neoglacial cooling and an increase in the sea-ice cover. At 3–2.8 ka a solar irradiance minimum may have triggered a rapid increase of the sea-ice occurrence that led to a stronger stratification of

CPD

9, 5037–5075, 2013

Water mass evolution of the Greenland Sea since lateglacial times

M. M. Telesiński et al.

Title Page

Abstract

Introduction

Conclusions

References

Tables

Figures

⏪

⏩

◀

▶

Back

Close

Full Screen / Esc

Printer-friendly Version

Interactive Discussion

Water mass evolution of the Greenland Sea since lateglacial times

M. M. Telesiński et al.

Title Page

Abstract

Introduction

Conclusions

References

Tables

Figures

⏪

⏩

◀

▶

Back

Close

Full Screen / Esc

Printer-friendly Version

Interactive Discussion

the upper water layers and, subsequently, to a weakening of deep convection in the Greenland Sea and of the AMOC. Then, an increase in AW inflow into the Nordic Seas led to the subsurface warming in the central Greenland Sea (site PS1878). Due to the relatively strong water stratification and presence of sea-ice (and thus the isolation of the subsurface water from the atmosphere and other water masses) subsurface temperatures rose to a level comparable with the Early Holocene thermal maximum at this site.

The comparison of the Greenland Sea records suggests insolation to be the primary driver controlling the regional palaeoceanographic evolution while the routing and intensity of AW inflow seems to control the spatial variability in the area. Other processes, including sea-ice formation, deep convection, freshwater discharges etc. also played an important role.

Acknowledgements. This work is a contribution to the CASE Initial Training Network funded by the European Community's 7th Framework Programme FP7 2007/2013, Marie-Curie Actions, under Grant Agreement No. 238111. We thank Katrine Husum for the help with performing the transfer function. We are grateful to Lulzim Haxhij for performing the stable isotope measurements and to the Leibniz Laboratory, Kiel University, and the Poznan Radiocarbon Laboratory for the AMS ^{14}C datings.

The service charges for this open access publication have been covered by a Research Centre of the Helmholtz Association.

References

- Andersen, C., Koç, N., Jennings, A. E., and Andrews, J. T.: Nonuniform response of the major surface currents in the Nordic Seas to insolation forcing: Implications for the Holocene climate variability, *Paleoceanography*, 19, PA2003, doi:10.1029/2002PA000873, 2004.
- Bauch, D. and Bauch, H. A.: Last glacial benthic foraminiferal $\delta^{18}\text{O}$ anomalies in the polar North Atlantic: A modern analogue evaluation, *J. Geophys. Res.*, 106, 9135–9143, 2001.

**Water mass evolution
of the Greenland Sea
since lateglacial
times**

M. M. Telesiński et al.

[Title Page](#)[Abstract](#)[Introduction](#)[Conclusions](#)[References](#)[Tables](#)[Figures](#)[⏪](#)[⏩](#)[◀](#)[▶](#)[Back](#)[Close](#)[Full Screen / Esc](#)[Printer-friendly Version](#)[Interactive Discussion](#)

Bauch, H. A. and Erlenkeuser, H.: Interpreting Glacial-Interglacial Changes in Ice Volume and Climate From Subarctic Deep Water Foraminiferal $\delta^{18}\text{O}$, in: Earth's Climate and Orbital Eccentricity: The Marine Isotope Stage 11 Question, Geoph. Monog. Series 137, edited by: Droxler, L. H., Poore, A. W., and Burckle, R. Z., American Geophysical Union, Washington, D.C., 87–102, 2003.

Bauch, H. A. and Weinelt, M. S.: Surface water changes in the Norwegian Sea during last deglacial and Holocene times, *Quaternary Sci. Rev.*, 16, 1115–1124, 1997.

Bauch, H. A., Erlenkeuser, H., Spielhagen, R. F., Struck, U., Matthiessen, J., Thiede, J., and Heinemeier, J.: A multiproxy reconstruction of the evolution of deep and surface waters in the subarctic Nordic seas over the last 30,000 yr, *Quaternary Sci. Rev.*, 20, 659–678, 2001.

Blaschek, M. and Renssen, H.: The Holocene thermal maximum in the Nordic Seas: the impact of Greenland Ice Sheet melt and other forcings in a coupled atmosphere–sea-ice–ocean model, *Clim. Past*, 9, 1629–1643, doi:10.5194/cp-9-1629-2013, 2013.

Bond, G. C., Kromer, B., Beer, J., Muscheler, R., Evans, M. N., Showers, W., Hoffmann, S., Lotti-Bond, R., Hajdas, I., and Bonani, G.: Persistent solar influence on North Atlantic climate during the Holocene, *Science*, 294, 2130–2136, doi:10.1126/science.1065680, 2001.

Broecker, W. S., Kennett, J. P., Flower, B. P., Teller, J. T., Trumbore, S., Bonani, G., and Wolffli, W.: Routing of meltwater from the Laurentide Ice Sheet during the Younger Dryas cold episode, *Nature*, 341, 318–321, 1989.

Broecker, W. S., Denton, G. H., Edwards, R. L., Cheng, H., Alley, R. B., and Putnam, A. E.: Putting the Younger Dryas cold event into context, *Quaternary Sci. Rev.*, 29, 1078–1081, doi:10.1016/j.quascirev.2010.02.019, 2010.

Carstens, J., Hebbeln, D., and Wefer, G.: Distribution of planktic foraminifera at the ice margin in the Arctic (Fram Strait), *Mar. Micropaleontol.*, 29, 257–269, 1997.

Clark, D. L. and Hanson, A.: Central Arctic Ocean sediment texture: A key to ice transport mechanism, in: *Glacial-marine sedimentation*, edited by: Molnia, B. F., Plenum Press, New York, 301–330, 1983.

Clark, P. U. and Mix, A. C.: Ice sheets and sea level of the Last Glacial Maximum, *Quaternary Sci. Rev.*, 21, 1–7, doi:10.1016/S0277-3791(01)00118-4, 2002.

Condron, A. and Winsor, P.: Meltwater routing and the Younger Dryas, *P. Natl. Acad. Sci. USA*, 109, 19928–19933, doi:10.1073/pnas.1207381109, 2012.

Water mass evolution of the Greenland Sea since lateglacial times

M. M. Telesiński et al.

[Title Page](#)

[Abstract](#)

[Introduction](#)

[Conclusions](#)

[References](#)

[Tables](#)

[Figures](#)

[⏪](#)

[⏩](#)

[◀](#)

[▶](#)

[Back](#)

[Close](#)

[Full Screen / Esc](#)

[Printer-friendly Version](#)

[Interactive Discussion](#)



Cronin, T. M., Dwyer, G. S., Farmer, J., Bauch, H. A., Spielhagen, R. F., Jakobsson, M., Nilsson, J., Briggs Jr., W. M., and Stepanova, A.: Deep Arctic Ocean warming during the last glacial cycle, *Nat. Geosci.*, 5, 631–634, doi:10.1038/ngeo1557, 2012.

Duplessy, J. C., Labeyrie, L. D., and Blanc, P. L.: Norwegian Sea Deep Water Variations over the Last Climatic Cycle: Paleo-Oceanographical Implications, in: *Long and Short Term Variability of Climate*, edited by: Wanner, H. and Siegenthaler, U., Springer, New York, 83–116, 1988.

Fisher, T. G. and Lowell, T. V.: Testing northwest drainage from Lake Agassiz using extant ice margin and strandline data, *Quatern. Int.*, 260, 106–114, doi:10.1016/j.quaint.2011.09.018, 2012.

Fronval, T. and Jansen, E.: Eemian and early Weichselian (140–60 ka) paleoceanography and paleoclimate in the Nordic seas with comparisons to Holocene conditions, *Paleoceanography*, 12, 443–462, 1997.

Giraudeau, J., Grelaud, M., Solignac, S., Andrews, J. T., Moros, M., and Jansen, E.: Millennial-scale variability in Atlantic water advection to the Nordic Seas derived from Holocene coccolith concentration records, *Quaternary Sci. Rev.*, 29, 1276–1287, doi:10.1016/j.quascirev.2010.02.014, 2010.

Hald, M., Andersson, C., Ebbesen, H., Jansen, E., Klitgaard-Kristensen, D., Risebrobakken, B., Salomonsen, G. R., Sarnthein, M., Sejrup, H. P., and Telford, R. J.: Variations in temperature and extent of Atlantic Water in the northern North Atlantic during the Holocene, *Quaternary Sci. Rev.*, 26, 3423–3440, doi:10.1016/j.quascirev.2007.10.005, 2007.

Hall, I. R., Bianchi, G. G., and Evans, J. R.: Centennial to millennial scale Holocene climate-deep water linkage in the North Atlantic, *Quaternary Sci. Rev.*, 23, 1529–1536, doi:10.1016/j.quascirev.2004.04.004, 2004.

Hansen, B. and Østerhus, S.: North Atlantic–Nordic Seas exchanges, *Prog. Oceanogr.*, 45, 109–208, doi:10.1016/S0079-6611(99)00052-X, 2000.

Hillaire-Marcel, C. and de Vernal, A.: Stable isotope clue to episodic sea ice formation in the glacial North Atlantic, *Earth Planet. Sc. Lett.*, 268, 143–150, doi:10.1016/j.epsl.2008.01.012, 2008.

Husum, K. and Hald, M.: Arctic planktic foraminiferal assemblages: Implications for subsurface temperature reconstructions, *Mar. Micropaleontol.*, 96–97, 38–47, doi:10.1016/j.marmicro.2012.07.001, 2012.

Water mass evolution of the Greenland Sea since lateglacial times

M. M. Telesiński et al.

[Title Page](#)

[Abstract](#)

[Introduction](#)

[Conclusions](#)

[References](#)

[Tables](#)

[Figures](#)

[⏪](#)

[⏩](#)

[◀](#)

[▶](#)

[Back](#)

[Close](#)

[Full Screen / Esc](#)

[Printer-friendly Version](#)

[Interactive Discussion](#)

Juggins, S.: C2, Version 1.7.2, Software for Ecological and Palaeoecological Data Analysis and Visualization, <http://www.campus.ncl.ac.uk/staff/Stephen.Juggins/index.html>, University of Newcastle, Newcastle upon Tyne, UK, 2011.

Marshall, J. and Schott, F.: Open-ocean convection: Observations, theory, and models, *Rev. Geophys.*, 37, 1–64, 1999.

Müller, J., Werner, K., Stein, R., Fahl, K., Moros, M., and Jansen, E.: Holocene cooling culminates in sea ice oscillations in Fram Strait, *Quaternary Sci. Rev.*, 47, 1–14, doi:10.1016/j.quascirev.2012.04.024, 2012.

Murton, J. B., Bateman, M. D., Dallimore, S. R., Teller, J. T., and Yang, Z.: Identification of Younger Dryas outburst flood path from Lake Agassiz to the Arctic Ocean, *Nature*, 464, 740–743, doi:10.1038/nature08954, 2010.

Nørgaard-Pedersen, N., Spielhagen, R. F., Erlenkeuser, H., Grootes, P. M., Heinemeier, J., and Knies, J.: Arctic Ocean during the Last Glacial Maximum: Atlantic and polar domains of surface water mass distribution and ice cover, *Paleoceanography*, 18, 1–19, doi:10.1029/2002PA000781, 2003.

Nürnberg, D., Wollenburg, I., Dethleff, D., Eicken, H., Kassens, H., Letzig, T., Reimnitz, E., and Thiede, J.: Sediments in Arctic sea ice: implications for entrainment, transport and release, *Mar. Geol.*, 104, 185–214, 1994.

Rasmussen, T. L. and Thomsen, E.: Stable isotope signals from brines in the Barents Sea: Implications for brine formation during the last glaciation, *Geology*, 37, 903–906, doi:10.1130/G25543A.1, 2009.

Rasmussen, T. L. and Thomsen, E.: Holocene temperature and salinity variability of the Atlantic Water inflow to the Nordic seas, *Holocene*, 20, 1223–1234, doi:10.1177/0959683610371996, 2010.

Reimer, P., Baillie, M., Bard, E., Bayliss, A., Beck, J. W., Blackwell, P. G., Bronk Ramsey, C., Buck, C. E., Burr, G. S., Edwards, R. L., Friedrich, M., Grootes, P. M., Guilderson, T. P., Hajdas, I., Heaton, T. J., Hogg, A. G., Hughen, K. A., Kaiser, K. F., Kromer, B., McCormac, F. G., Manning, S. W., Reimer, R. W., Richards, D. A., Southon, J. R., Talamo, S., Turney, C. S. M., van der Plicht, J., and Weyhenmeyer, C. E.: IntCal09 and Marine09 radiocarbon age calibration curves, 0–50,000 years cal BP, *Radiocarbon*, 51, 1111–1150, 2009.

Renssen, H., Goosse, H., and Muscheler, R.: Coupled climate model simulation of Holocene cooling events: oceanic feedback amplifies solar forcing, *Clim. Past*, 2, 79–90, doi:10.5194/cp-2-79-2006, 2006.

Water mass evolution of the Greenland Sea since lateglacial times

M. M. Telesiński et al.

[Title Page](#)

[Abstract](#)

[Introduction](#)

[Conclusions](#)

[References](#)

[Tables](#)

[Figures](#)

[⏪](#)

[⏩](#)

[◀](#)

[▶](#)

[Back](#)

[Close](#)

[Full Screen / Esc](#)

[Printer-friendly Version](#)

[Interactive Discussion](#)

- Risebrobakken, B., Dokken, T., Smedsrud, L. H., Andersson, C., Jansen, E., Moros, M., and Ivanova, E. V.: Early Holocene temperature variability in the Nordic Seas: The role of oceanic heat advection versus changes in orbital forcing, *Paleoceanography*, 26, PA4206, doi:10.1029/2011PA002117, 2011.
- 5 Sarnthein, M., Jansen, E., Weinelt, M., Arnold, M., Duplessy, J. C., Erlenkeuser, H., Flatøy, A., Johannessen, G., Johannessen, T., Jung, S., Koc, N., Labeyrie, L., Maslin, M., Pflaumann, U., and Schulz, H.: Variations in Atlantic surface ocean paleoceanography, 50°–80° N: A time-slice record of the last 30,000 years, *Paleoceanography*, 10, 1063–1094, 1995.
- 10 Sarnthein, M., van Kreveld, S., Erlenkeuser, H., Grootes, P. M., Kucera, M., Pflaumann, U., and Schulz, M.: Centennial-to-millennial-scale periodicities of Holocene climate and sediment injections off the western Barents shelf, 75° N. *Boreas*, 32, 447–461, doi:10.1080/03009480310003351, 2003.
- Spielhagen, R. F. and Erlenkeuser, H.: Stable oxygen and carbon isotopes in planktic foraminifers from Arctic Ocean surface sediments: Reflection of the low salinity surface water layer, *Mar. Geol.*, 119, 227–250, doi:10.1016/0025-3227(94)90183-X, 1994.
- 15 Spielhagen, R. F., Baumann, K.-H., Erlenkeuser, H., Nowaczyk, N. R., Nørgaard-Pedersen, N., Vogt, C., and Weiel, D.: Arctic Ocean deep-sea record of northern Eurasian ice sheet history, *Quaternary Sci. Rev.*, 23, 1455–1483, doi:10.1016/j.quascirev.2003.12.015, 2004.
- Spielhagen, R. F., Werner, K., Aagaard-Sørensen, S., Zamelczyk, K., Kandiano, E., Budeus, G., Husum, K., Marchitto, T. M., and Hald, M.: Enhanced Modern Heat Transfer to the Arctic by Warm Atlantic Water, *Science*, 331, 450–453, doi:10.1126/science.1197397, 2011.
- 20 Stanford, J. D., Rohling, E. J., Bacon, S., Roberts, A. P., Grousset, F. E., and Bolshaw, M.: A new concept for the paleoceanographic evolution of Heinrich event 1 in the North Atlantic, *Quaternary Sci. Rev.*, 30, 1047–1066, doi:10.1016/j.quascirev.2011.02.003, 2011.
- 25 Stern, J. V. and Lisiecki, L. E.: North Atlantic circulation and reservoir age changes over the past 41,000 years, *Geophys. Res. Lett.*, 40, 3693–3697, doi:10.1002/grl.50679, 2013.
- Stuiver, M. and Reimer, P. J.: Radiocarbon calibration program, *Radiocarbon*, 35, 215–230, 1993.
- Swift, J.: The Arctic Waters, in: *The Nordic Seas*, edited by: Hurdle, B., Springer, New York, 129–151, 1986.
- 30 Telesiński, M. M., Spielhagen, R. F., and Lind, E. M.: A high-resolution Late Glacial and Holocene paleoceanographic record from the Greenland Sea, *Boreas*, submitted, 2013.

Water mass evolution of the Greenland Sea since lateglacial times

M. M. Telesiński et al.

[Title Page](#)

[Abstract](#)

[Introduction](#)

[Conclusions](#)

[References](#)

[Tables](#)

[Figures](#)

[⏪](#)

[⏩](#)

[◀](#)

[▶](#)

[Back](#)

[Close](#)

[Full Screen / Esc](#)

[Printer-friendly Version](#)

[Interactive Discussion](#)



- Teller, J. T., Boyd, M., Yang, Z., Kor, P. S. G., and Mokhtari Fard, A.: Alternative routing of Lake Agassiz overflow during the Younger Dryas: new dates, paleotopography, and a re-evaluation, *Quaternary Sci. Rev.*, 24, 1890–1905, doi:10.1016/j.quascirev.2005.01.008, 2005.
- 5 Thiede, J. and Hempel, G.: The Expedition ARKTIS-VII/1 of RV “POLARSTERN” in 1990, *Ber. Polarforsch.*, 80, 137 pp., 1991.
- Thornalley, D. J. R., Elderfield, H., and McCave, I. N.: Intermediate and deep water paleoceanography of the northern North Atlantic over the past 21,000 years, *Paleoceanography*, 25, 1–17, doi:10.1029/2009PA001833, 2010.
- 10 Vogelsang, E.: Paläo-Ozeanographie des Europäischen Nordmeeres an Hand stabiler Kohlenstoff- und Sauerstoffisotope (Paleoceanography of the Nordic seas on the basis of stable carbon and oxygen isotopes), *Berichte aus dem Sonderforschungsbereich 313*, Nr. 23, Univ. Kiel, Kiel, 1990.
- Waelbroeck, C., Duplessy, J. C., Michel, E., Labeyrie, L., Paillard, D., and Duprat, J.: The timing of the last deglaciation in North Atlantic climate records. *Nature*, 412, 724–7, doi:10.1038/35089060, 2001.
- 15 Werner, K., Spielhagen, R. F., Bauch, D., Christian Hass, H., and Kandiano, E.: Atlantic Water advection versus sea-ice advances in the eastern Fram Strait during the last 9 ka: Multiproxy evidence for a two-phase Holocene, *Paleoceanography*, 28, 283–295, doi:10.1002/palo.20028, 2013.
- 20

Water mass evolution of the Greenland Sea since lateglacial times

M. M. Telesiński et al.

Table 1. Cores used in the study.

Core	Latitude	Longitude	Water depth (m)	Core type	Core length (cm)
PS1878-2	73°15.1 N	9°00.9 W	3038	BC ¹	27
PS1878-3	73°15.3 N	9°00.7 W	3048	KC ²	113
PS1894-7	75°48.8 N	8°15.5 W	1992	BC ¹	42
PS1906-1	76°50.5 N	2°09.0 W	2990	BC ¹	33
PS1910-1	75°37.0 N	1°19.0 E	2448	BC ¹	33

¹ BC – giant box core, ² KC – kasten core.

Title Page

Abstract

Introduction

Conclusions

References

Tables

Figures

⏪

⏩

◀

▶

Back

Close

Full Screen / Esc

Printer-friendly Version

Interactive Discussion

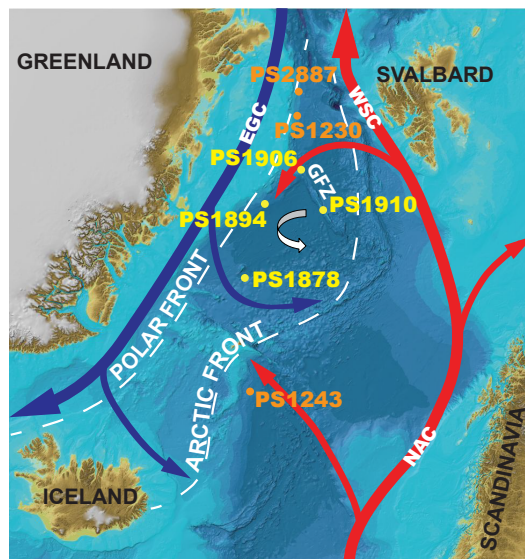


Fig. 1. Present day surface water circulation in the Nordic Seas. Cores used in this study are marked with yellow dots; other cores mentioned in text are marked with orange dots. Red arrows indicate Atlantic Water, blue arrows – Polar Water, white broken lines – oceanographic fronts. White arrow – present-day deep convection (Marshall and Schott, 1999). EGC – East Greenland Current, NAC – North Atlantic Current, WSC – West Spitsbergen Current, GFZ – Greenland Fracture Zone. Bathymetry from The International Bathymetric Chart of the Arctic Ocean (<http://www.ibcao.org>, 2012).

Water mass evolution of the Greenland Sea since lateglacial times

M. M. Telesiński et al.

Title Page

Abstract

Introduction

Conclusions

References

Tables

Figures



Back

Close

Full Screen / Esc

Printer-friendly Version

Interactive Discussion



Water mass evolution of the Greenland Sea since lateglacial times

M. M. Telesiński et al.

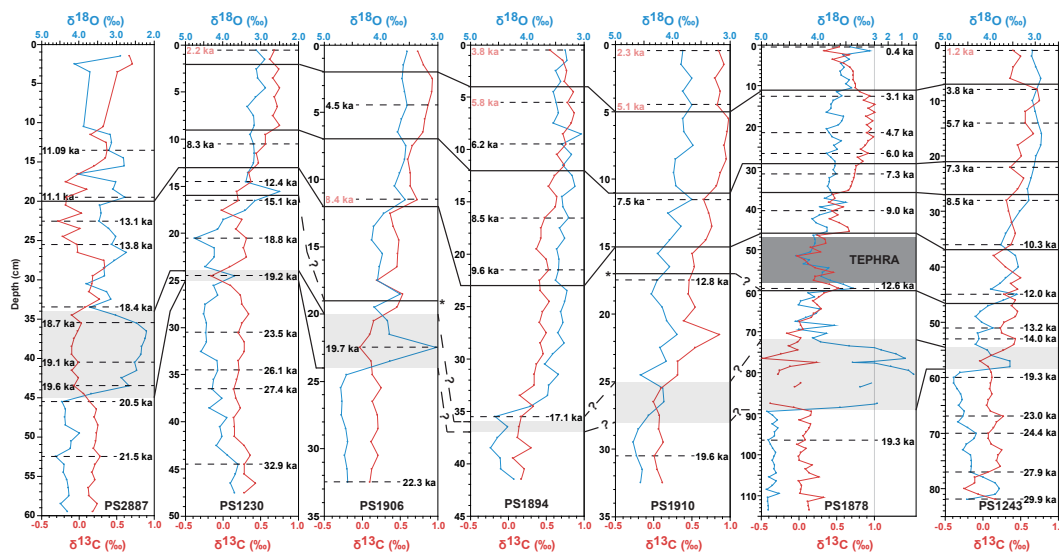


Fig. 2. Planktic oxygen and carbon stable isotope records of cores from the Nordic Seas and suggested correlation between them. Calibrated AMS ^{14}C dates are shown. Dates excluded from the correlation are marked with pale red.

Title Page

Abstract

Introduction

Conclusions

References

Tables

Figures



Back

Close

Full Screen / Esc

Printer-friendly Version

Interactive Discussion

Water mass evolution of the Greenland Sea since lateglacial times

M. M. Telesiński et al.

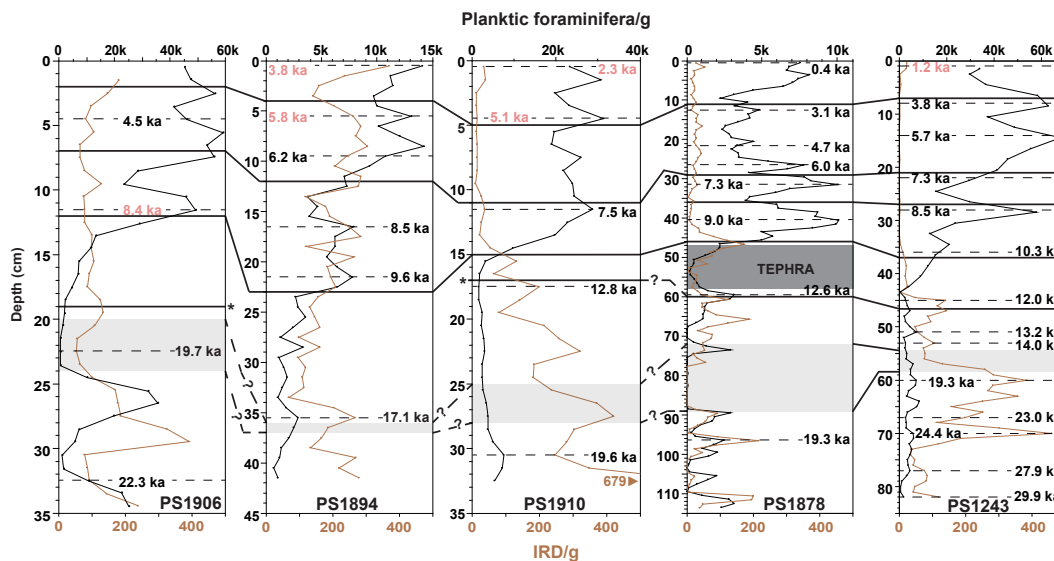


Fig. 3. Planktic foraminifera and IRD abundance (per 1 g dry sediment) of cores used in this study and core PS1243. Correlation and ages as in Fig. 2.

Title Page

Abstract

Introduction

Conclusions

References

Tables

Figures



Back

Close

Full Screen / Esc

Printer-friendly Version

Interactive Discussion

Water mass evolution of the Greenland Sea since lateglacial times

M. M. Telesiński et al.

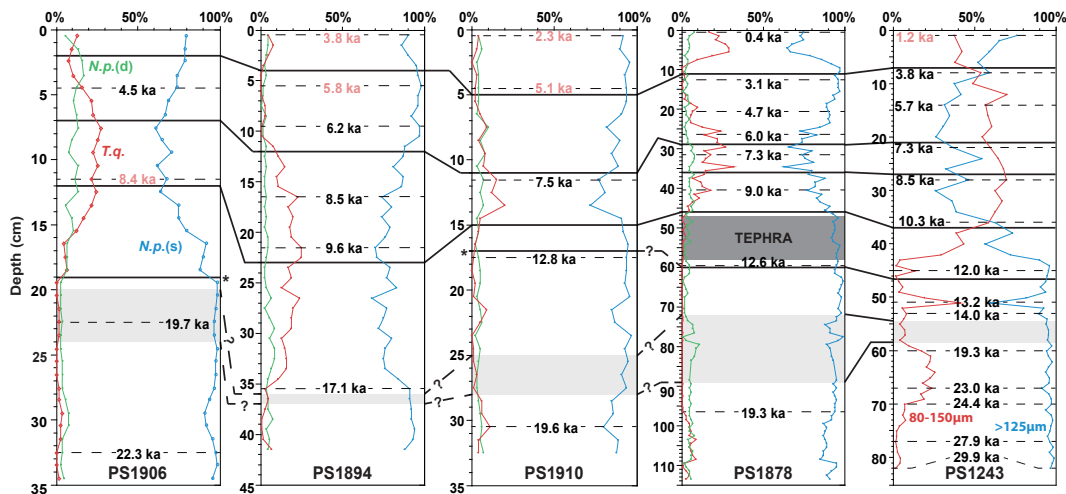


Fig. 4. Relative abundances of the three most common planktic foraminifera species in cores used in this study and core PS1243. *N.p. (s)* – *N. pachyderma* (sin), *N.p. (d)* – *N. pachyderma* (dex), *T.q.* – *T. quinqueloba*. Correlation and ages as in Fig. 2. Mark the different size fractions used in core PS1243.

[Title Page](#)
[Abstract](#)
[Introduction](#)
[Conclusions](#)
[References](#)
[Tables](#)
[Figures](#)
[Back](#)
[Close](#)
[Full Screen / Esc](#)
[Printer-friendly Version](#)
[Interactive Discussion](#)

Water mass evolution of the Greenland Sea since lateglacial times

M. M. Telesiński et al.

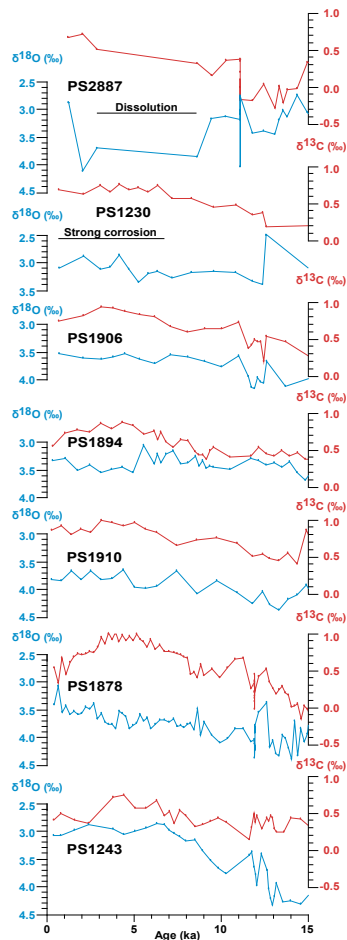


Fig. 5. Planktic oxygen and carbon stable isotope records of cores from the Nordic Seas vs. age (since 15 ka).

[Title Page](#)
[Abstract](#)
[Introduction](#)
[Conclusions](#)
[References](#)
[Tables](#)
[Figures](#)
[◀](#)
[▶](#)
[◀](#)
[▶](#)
[Back](#)
[Close](#)
[Full Screen / Esc](#)
[Printer-friendly Version](#)
[Interactive Discussion](#)

Water mass evolution of the Greenland Sea since lateglacial times

M. M. Telesiński et al.

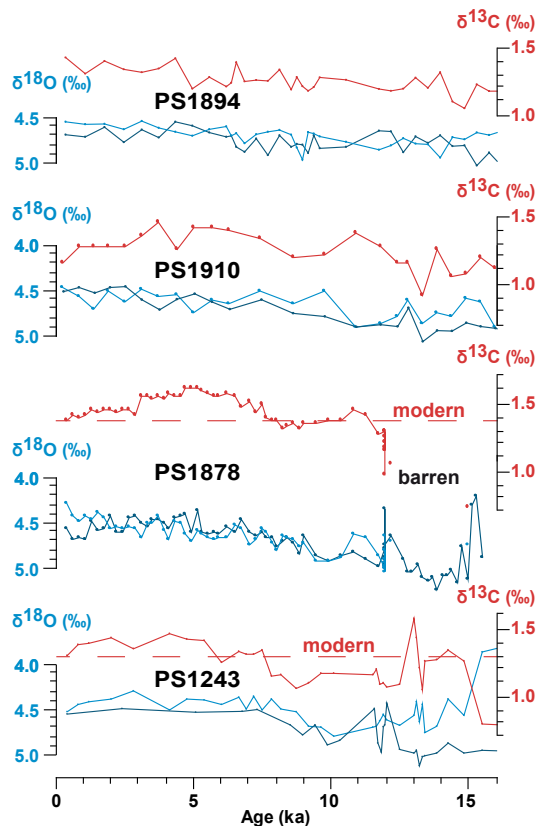


Fig. 6. Benthic oxygen (light and dark blue for *C. wuellerstorfi* and *O. umbonatus*, respectively) and carbon (red, *C. wuellerstorfi*) stable isotope records (in ‰ vs. PDB) of cores PS1894, PS1910, PS1878 and PS1243 vs. age (since 16 ka). Broken lines in PS1878 and PS1243 mark the modern (coretop) $\delta^{13}\text{C}$ values of *C. wuellerstorfi* from the central Greenland Sea and site PS1243, respectively (Bauch and Erlenkeuser, 2003).

Water mass evolution of the Greenland Sea since lateglacial times

M. M. Telesiński et al.

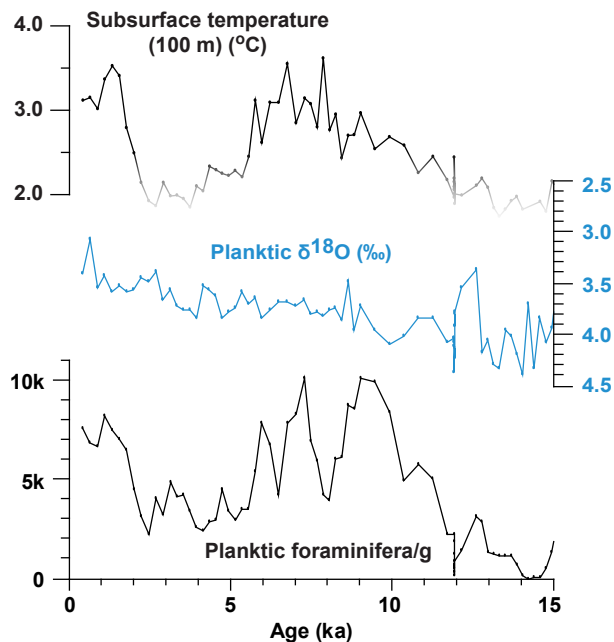


Fig. 7. Absolute subsurface temperatures calculated using transfer function on planktic foraminifera from core PS1878 plotted against planktic oxygen isotope and total planktic foraminiferal abundance records. Temperatures below 2 °C should be considered uncertain.

[Title Page](#)[Abstract](#)[Introduction](#)[Conclusions](#)[References](#)[Tables](#)[Figures](#)[◀](#)[▶](#)[◀](#)[▶](#)[Back](#)[Close](#)[Full Screen / Esc](#)[Printer-friendly Version](#)[Interactive Discussion](#)

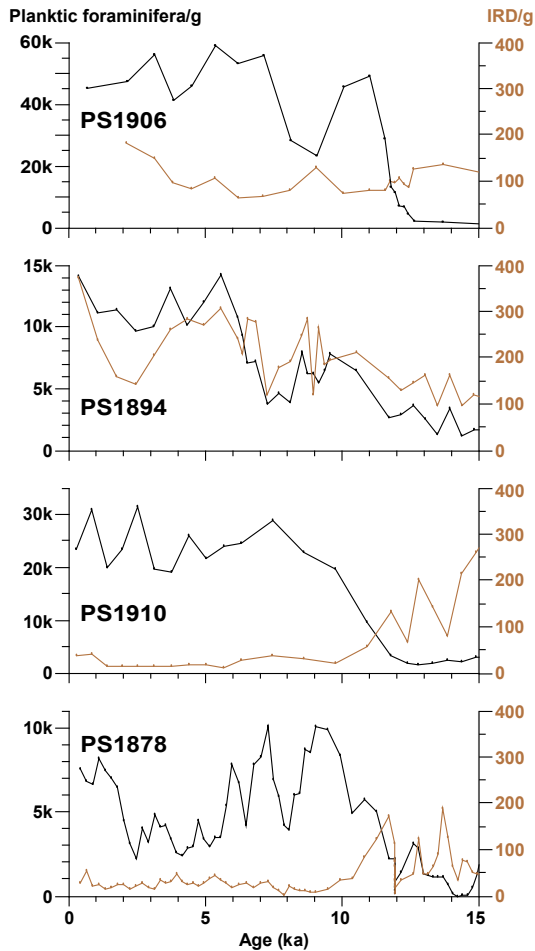


Fig. 8. Planktic foraminifera and IRD abundance (per 1 g dry sediment) of cores used in this study vs. age (since 15 ka).

Water mass evolution of the Greenland Sea since lateglacial times

M. M. Telesiński et al.

[Title Page](#)

[Abstract](#) | [Introduction](#)

[Conclusions](#) | [References](#)

[Tables](#) | [Figures](#)

[⏪](#) | [⏩](#)

[◀](#) | [▶](#)

[Back](#) | [Close](#)

[Full Screen / Esc](#)

[Printer-friendly Version](#)

[Interactive Discussion](#)



Water mass evolution of the Greenland Sea since lateglacial times

M. M. Telesiński et al.

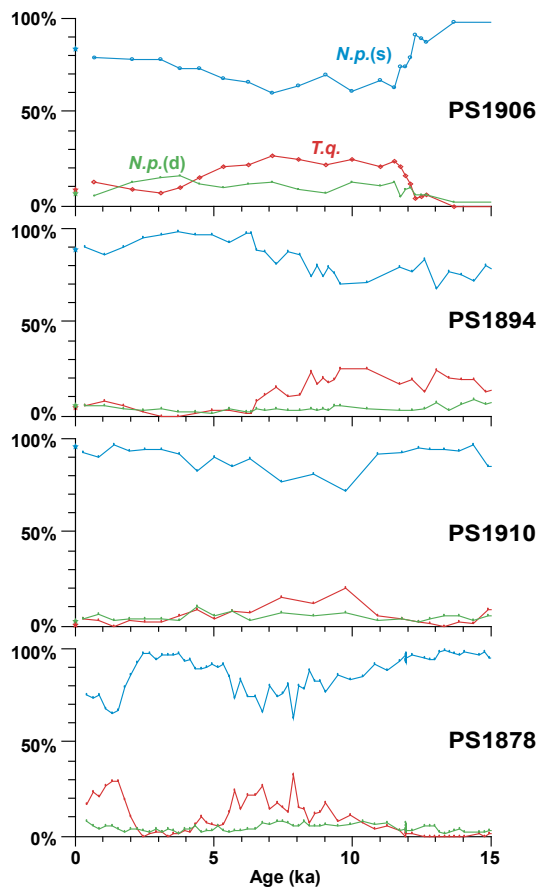


Fig. 9. Relative abundance of the three most common planktic foraminifera species in cores used in this study vs. age (since 15 ka). Abbreviations as in Fig. 4. Asterisks mark the modern (coretop) values (own data).

[Title Page](#)
[Abstract](#)
[Introduction](#)
[Conclusions](#)
[References](#)
[Tables](#)
[Figures](#)
[◀](#)
[▶](#)
[◀](#)
[▶](#)
[Back](#)
[Close](#)
[Full Screen / Esc](#)
[Printer-friendly Version](#)
[Interactive Discussion](#)